



OPEN ACCESS

EDITED BY

Xin Wang,
National Institutes of Health (NIH),
United States

REVIEWED BY

Zhuoyu Wen,
University of Texas Southwestern Medical
Center, United States
Shuiping Liu,
Hangzhou Normal University, China

*CORRESPONDENCE

Chengzhi Huang
✉ huangchengzhi93@hotmail.com
Xueqing Yao
✉ syyaoxueqing@scut.edu.cn

†These authors have contributed
equally to this work

RECEIVED 08 February 2023

ACCEPTED 05 May 2023

PUBLISHED 06 June 2023

CITATION

Li H, Feng X, Hu Y, Wang J, Huang C and
Yao X (2023) Development of a prognostic
model based on ferroptosis-related genes
for colorectal cancer patients and
exploration of the biological functions of
NOS2 *in vivo* and *in vitro*.
Front. Oncol. 13:1133946.
doi: 10.3389/fonc.2023.1133946

COPYRIGHT

© 2023 Li, Feng, Hu, Wang, Huang and Yao.
This is an open-access article distributed
under the terms of the [Creative Commons
Attribution License \(CC BY\)](https://creativecommons.org/licenses/by/4.0/). The use,
distribution or reproduction in other
forums is permitted, provided the original
author(s) and the copyright owner(s) are
credited and that the original publication in
this journal is cited, in accordance with
accepted academic practice. No use,
distribution or reproduction is permitted
which does not comply with these terms.

Development of a prognostic model based on ferroptosis-related genes for colorectal cancer patients and exploration of the biological functions of NOS2 *in vivo* and *in vitro*

Hongming Li^{1,2,3†}, Xiaochuang Feng^{3†}, Yong Hu^{2†},
Junjiang Wang^{1,2†}, Chengzhi Huang^{4*} and Xueqing Yao^{1,2*}

¹The Second School of Clinical Medicine, Southern Medical University, Guangzhou, Guangdong, China, ²Department of Gastrointestinal Surgery, Department of General Surgery, Guangdong Provincial People's Hospital (Guangdong Academy of Medical Sciences), Southern Medical University, Guangzhou, China, ³Department of Colorectal Surgery, Guangdong Provincial Hospital of Chinese Medicine, Guangzhou, Guangdong, China, ⁴School of Bioscience and Bioengineering, South China University of Technology, Guangzhou, Guangdong, China

Background: Ferroptosis is involved in many malignant tumors and has been implicated in important mechanisms of colorectal cancer (CRC) suppression. However, the prognostic and predictive values of the ferroptosis activation pattern in CRC patients have not been noted. Here, we aimed to construct and validate a prediction model based on ferroptosis-related genes (FRGs) for CRC patients and investigated the expression pattern and biological function of the most significantly altered gene.

Methods: A total of 112 FRGs were obtained from the FerrDb website, and the clinical characteristics of 545 CRC patients and their global gene expression profiles were downloaded from The Cancer Genome Atlas (TCGA) database. Survival-related FRGs were identified by Cox proportional hazards regression analysis. Finally, the expression pattern and biological function of NOS2, the most implicated gene was explored *in vitro* and *in vivo*.

Results: The prediction model was established based on 8 FRGs. Patients in the high- or low-risk group were stratified based on the median risk value calculated by our model, and patients in the high-risk group experienced poor overall survival ($p < 0.01$). Further validation demonstrated that the FRG model acted as an independent prognostic indicator for CRC patients (HR=1.428, 95% CI, 1.341-1.627; $p < 0.001$). The area under the receiver operating characteristic (ROC) curve (AUC) for 5-year survival was 0.741. NOS2 was one of the most significantly affected FRGs and was highly expressed in malignant tissue, but it inhibited tumor growth and induced tumor cell death *in vitro* and *in vivo*, possibly by repressing the NF- κ B pathway.

Conclusion: Our study revealed that FRGs have potential prognostic value in CRC patients and that NOS2 suppresses tumor progression, providing a novel therapeutic target for CRC treatment based on ferroptosis.

KEYWORDS

colorectal cancer, ferroptosis, prognostic model, gene, NOS2

Introduction

CRC is the third most frequently diagnosed malignant tumor worldwide, accounting for approximately 10% of all cancers and leading to almost 9×10^5 deaths annually (1, 2). The incidence of CRC has been increasing over recent decades, and it is foreseeable that new cases will reach 2.5 million in 2035, and the treatment and management of CRC have become more difficult due to the increase in drug resistance (3–5). However, guiding prognostication and treatment decision-making with biomarkers would provide promising therapeutic targets for CRC (6).

Ferroptosis is an important and recently identified form of nonapoptotic cell death driven by iron-dependent lipid peroxidation that was first proposed in 2012 (7). Emerging evidence has gradually indicated the tumor-suppressive consequence of ferroptosis through cysteine deprivation and reactive oxygen species (ROS) production by p53 (8, 9). To date, ferroptosis has been shown to affect the immune microenvironment, metabolism, and cell proliferation in CRC and acts downstream of chemotherapy and targeted therapy in KRAS-mutated CRC cells (10–12). However, the diagnostic and prognostic values and underlying biological mechanisms involved in ferroptosis remain unclear in CRC.

As shown in previous studies, NOS2 (Enzyme Nitric Oxide Synthase 2) might act in the process of ferroptosis and have implications for patient stratification for prognosis (13, 14). NOS2 is a calcium-independent and inducible enzyme that contributes to the production of NO in cells; therefore, it is related to immune response facilitation, the vascular relaxation function, and inflammation (15, 16). In many types of cancer, the mechanisms by which NOS2 is involved are complex and poorly defined, with both promoting and inhibiting functions having been described (15, 17, 18). Several studies have addressed the mechanisms by which NOS2 promotes tumor progression by p53 and TNF α interactions within the tumor microenvironment (19, 20). However, NOS2 is essential for T cell immunotherapies to destroy tumors (21).

Our study analyzed the correlation between the expression pattern of FRGs and the survival of 545 CRC patients from the TCGA database, and a prognostic model based on the risk score of 8 FRGs identified by multivariate Cox regression analysis

was established. Furthermore, we explored the expression pattern and the tumor suppressive role and mechanism of NOS2, which was one of the most significantly affected gene in our model.

Materials and methods

Data sources

A total of 112 FRGs, including ferroptosis drivers, suppressors and markers, were obtained from the FerrDB website (<http://www.zhounan.org/ferrdb/>). We downloaded the mRNA expression data and clinical characteristics of 545 patients diagnosed with CRC from The Cancer Genome Atlas (TCGA) database (<https://www.cancer.gov/>).

Identification of differentially expressed FRGs and enrichment analysis

We ran the edgeR package to identify differentially expressed FRGs (fold change >2, adjusted p -value < 0.05) between CRC and normal tissues. Then, we used a parallel box diagram to visualize these eligible FRGs and conducted Gene Ontology (GO) and Kyoto Encyclopedia of Genes and Genomes (KEGG) analyses for gene functional enrichment analyses. “GO plot” and “KEGG plot” were used to visualize the results.

Establishment of the individualized prognostic model based on FRGs

We performed univariate Cox regression analysis to select the significant survival-related FRGs and avoid false positives and overfitting of the model by LASSO regression analysis. Next, we used multivariate Cox regression analysis to further identify FRGs that could independently predict survival. Finally, the prognostic model was established according to the relative expression levels of the screened FRGs and weighted according to regression coefficients (β) with a multivariate Cox regression model. The equation was as follows:

Abbreviations: CRC, Colorectal cancer; FRGs, Ferroptosis-related genes; ROS, Reactive oxygen species; NOS2, Enzyme nitric oxide synthase 2; MTT, 3-(4, 5-dimethyl-thiaziazolo-2-yl)-2, 5-di-phenyltetrazolium bromide.

$$\begin{aligned} \text{Risk score} = & \beta_{\text{gene}(1)} \times \text{FRGexpression}(1) + \beta_{\text{gene}(2)} \\ & \times \text{FRGexpression}(2) + \dots + \beta_{\text{gene}(n)} \\ & \times \text{FRGexpression}(n) \end{aligned}$$

Calculating survival and the risk score

According to the median risk score, CRC patients were divided into the high- or low-risk group. Kaplan-Meier curves were generated to analyze the overall survival (OS) times between the two groups, and a time-dependent receiver operating characteristic (ROC) curve was used to evaluate the accuracy of the prediction model. Then, we drew a nomogram to demonstrate the predictive probability and observation rate of five-year OS in CRC patients.

Western blot analysis and quantitative real-time PCR

We used RIPA buffer (Amresco, America) to lyse cells and tissues, separated total proteins by 10% SDS-PAGE (Amresco, America) and transferred them to PVDF membranes. All membranes were incubated overnight with primary antibodies at 4°C and with the HRP-conjugated secondary antibody at room temperature for 1 h. All western blot results were quantified by software Image J (v1.8.0).

For qRT-PCR, total mRNA was extracted from tumor cells or tumor tissues using TRIzol reagent and reverse transcribed into cDNA with a PrimeScript RT-PCR Kit. cDNA was amplified using SYBRTM Premix Ex TaqTM (TaKaRa, Japan) on a LightCycler 96 Detection System (Roche). GAPDH CT values were used for normalization.

MTT proliferation and clonogenic assays

For the MTT (3-(4, 5-dimethyl-thiaziazolo-2-yl)-2, 5-diphenyltetrazolium bromide) proliferation assay, transfected cells (1×10^3 cells per well) were seeded onto 96-well plates. After 24 h, we performed an MTT assay at fixed time points every day. For the clonogenic assay, 500 cells were cultivated per well into 6-well plates and maintained in RPMI 1640 medium with 10% fetal bovine serum at 37°C for 7 days.

In vivo subcutaneous xenograft models

All nude mice were purchased from Guangdong Medical Laboratory Animal Center. NOS2-overexpressing and control cell lines were transplanted subcutaneously into the bilateral flanks, and appropriate care was given to these animals. Tumor volume $[(\text{length} \times \text{width}^2)/2]$ was measured every 3 days, and all mice were sacrificed 21 days after injection.

Statistical analysis

All statistical analyses were performed using GraphPad Prism 8.0 and R 3.6.2. The R package edgeR was used for differential expression analysis, and then univariate LASSO and multivariate Cox regression analyses were performed to identify FRGs associated with prognosis and further introduced into the prognostic model. Differences in OS between CRC patients in the high-risk group and low-risk group were generated with the Kaplan-Meier method. The R package “survivalROC” was run to generate the ROC curve and the corresponding area under the ROC curve (AUC) for model evaluation. Relevant R packages used for statistical analysis referenced the method in (22).

Data are shown as the mean \pm SD, and all tests were considered statistically significant only when $p < 0.05$ was achieved.

Results

Differentially expressed FRGs in CRC and functional enrichment

First, we downloaded RNA-seq and clinical data from 646 CRC tissue samples and 68 normal colorectal mucosa specimens (Paired colon samples were from partial colon resection for carcinoma) from the TCGA database. Altogether, 545 CRC patients with follow-up data were eligible (Table 1). A total of 112 FRGs were accessed from the FerrDB website (Figure 1), and 61 genes (40 upregulated and 21 downregulated) were obtained under the criteria $\text{FDR} < 0.05$ and $\log_2(\text{fold change}) > 1$ (Figures 2A, B). Box plot graph showing these differential genes expression between normal and tumor tissues (Figure 2C). These differentially expressed FRGs were then subjected to functional enrichment analysis, and the top 28 GO terms and 8 KEGG pathways are visualized in Figures 2D, E. The top ranked pathways according to enrichment score were “Ferroptosis” and “Response to toxic substance”.

Identification of prognostic FRGs and construction of a predictive model

We selected the above 61 FRGs for further exploration and performed univariate Cox regression analysis. The results revealed that 14 differentially expressed FRGs were significantly correlated with OS (Table 2). Then, we conducted LASSO regression analysis to narrow the scope and avoid false positives and ultimately identified 8 FRGs independently associated with survival in CRC patients by multivariate Cox regression to construct a predictive model (Supplementary Table 1). A heatmap of the expression profiles of 8 FRGs is shown in Figure 3A.

According to the model, 545 patients were classified into the high- or low-risk group based on the median risk scores [Risk score = $-0.144 \times \text{NOS2 expression} + 0.723 \times \text{DRD4 expression} + (-0.561) \times \text{STAT3 expression} + 1.208 \times \text{LINC0036 expression} + 0.431 \times$

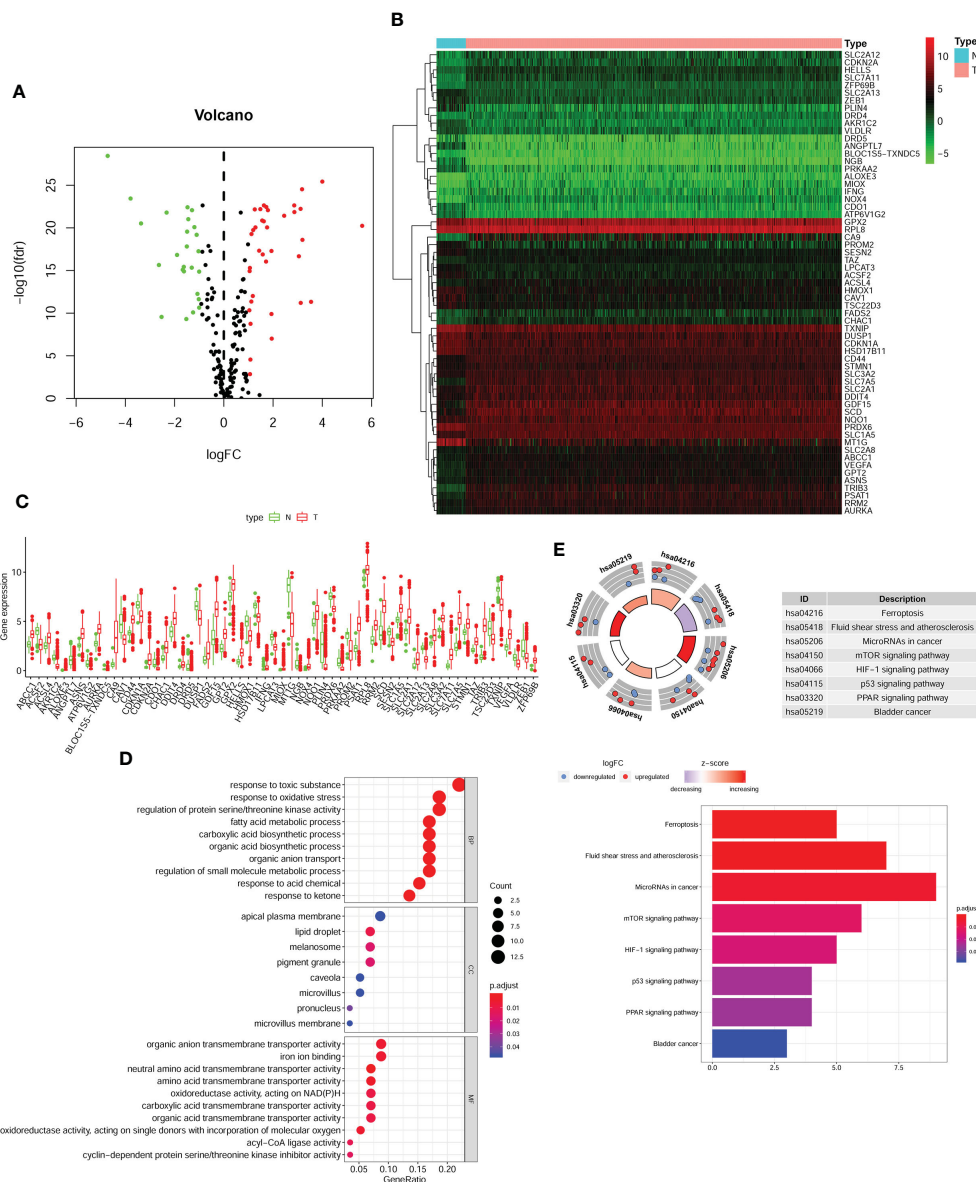


FIGURE 2 Differentially FRGs expressed in CRC and functional enrichment. Volcano plot (A), heatmap (B) and expression bar chart (C) showing the 61 differentially expressed FRGs in CRC tissues compared with normal tissue. The red dots represented significantly up-regulated FRGs, green dots stood for FRGs with significantly down-regulated and black dots stood for no significant differences FRGs. The GO analysis (D) and KEGE analysis (E) for molecular functions and potential pathways for differentially expressed FRGs involved in.

TABLE 2 Fourteen prognosis-related genes obtained based on univariate COX regression analysis.

Gene symbol	Hazard ratio	95%CI	p-Value
HSPB1	1.228	1.002–1.504	0.048
DDIT3	1.314	1.022–1.690	0.033
NOS2	0.852	v0.747–0.973	0.018
DRD4	1.719	1.162–2.542	0.007
STAT3	0.616	0.390–0.975	0.039
LINC00336	4.285	1.352–13.578	0.013

(Continued)

TABLE 2 Continued

Gene symbol	Hazard ratio	95%CI	p-Value
NOX4	1.612	1.015–2.561	0.043
ATP6V1G2	6.506	1.986–21.315	0.002
SLC2A3	1.348	1.102–1.649	0.004
JDP2	2.214	1.386–3.539	<0.001
DUOX1	1.800	1.177–2.752	0.007
SLC2A6	1.459	1.061–2.006	0.020
ISCU	1.865	1.043–3.334	0.036
ALOX12	2.561	1.196–5.482	0.015

NOS2 suppresses tumor proliferation *in vitro*

To further explore the biological functions of NOS2 in CRC, we first detected endogenous NOS2 expression in 11 CRC cell lines

through qRT-PCR and western blot (Figures 6A, B). According to the results, NOS2 was relatively highly expressed in HCT116 and SW480 cells and weakly expressed in SW620 and CACO2 cells. Thus, we generated HCT116 and SW480 cell lines stably overexpressing NOS2 and SW620 and CACO2 cell lines with

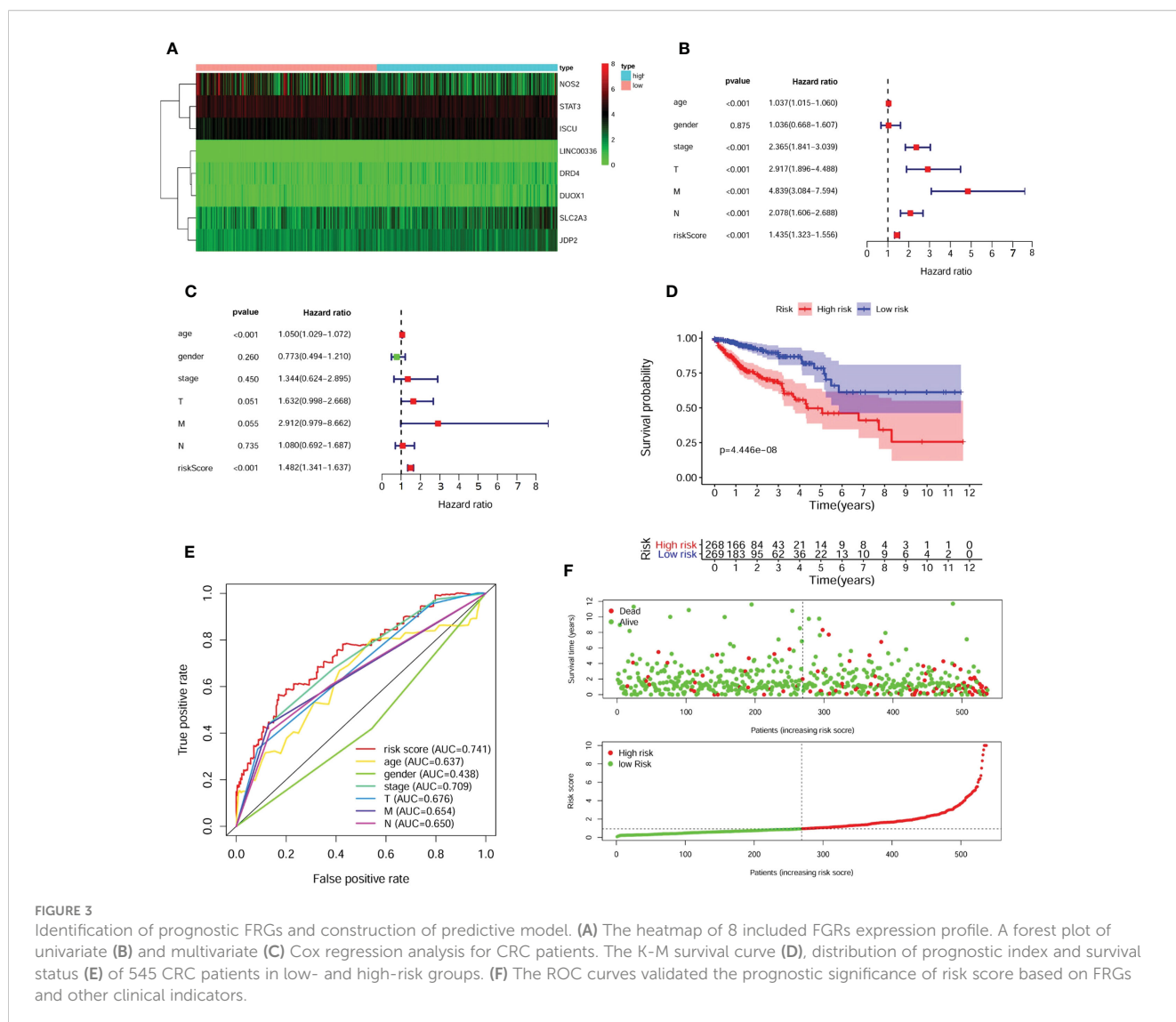


FIGURE 3

Identification of prognostic FRGs and construction of predictive model. (A) The heatmap of 8 included FRGs expression profile. A forest plot of univariate (B) and multivariate (C) Cox regression analysis for CRC patients. The K-M survival curve (D), distribution of prognostic index and survival status (E) of 545 CRC patients in low- and high-risk groups. (F) The ROC curves validated the prognostic significance of risk score based on FRGs and other clinical indicators.

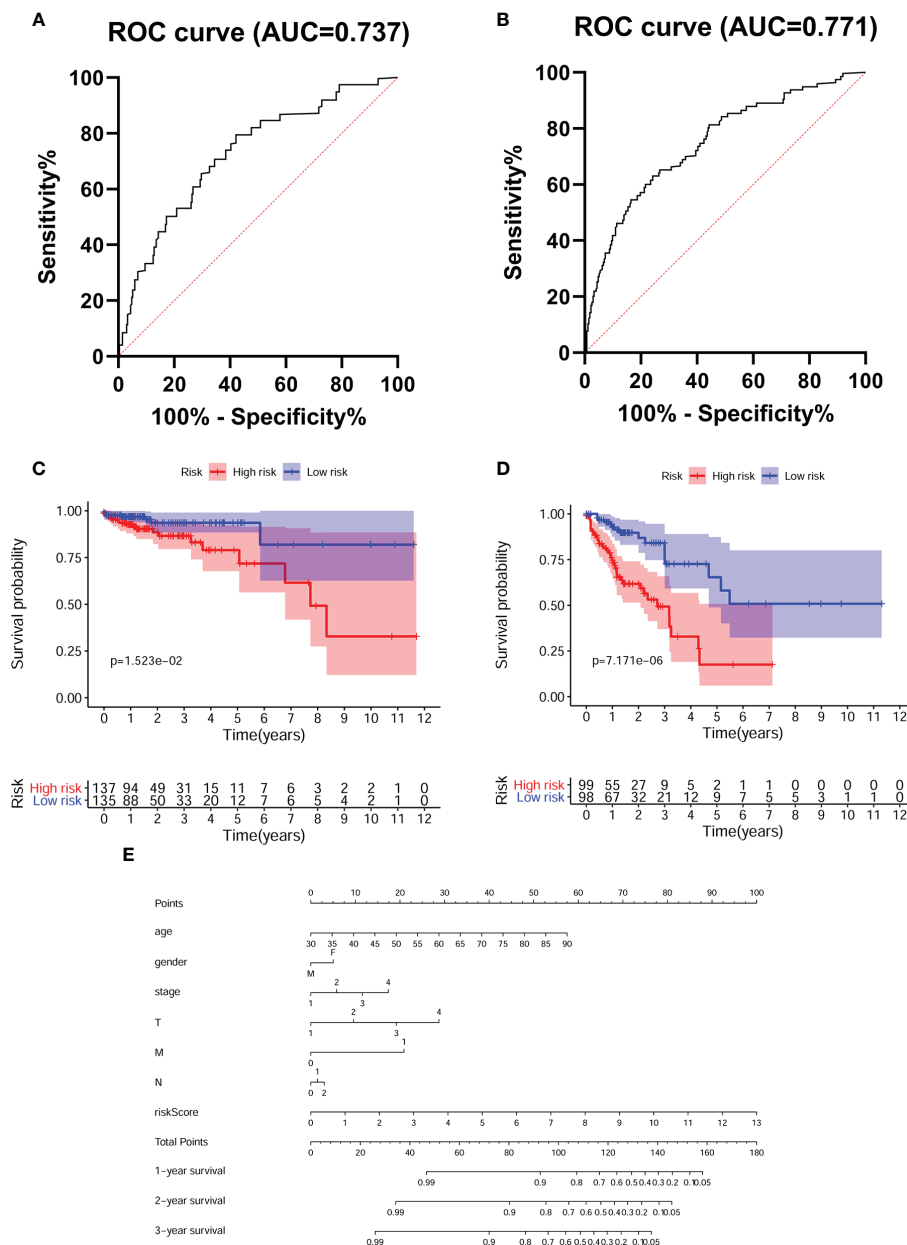


FIGURE 4 Evaluated the accuracy of the predictive model. Tumor stage-dependent ROC curve analysis (A).I/II; (B) III/IV for survival prediction based on the model. K-M survival curves for CRC patients with different tumor stage (C).I/II; (D) III/IV in low- and high- risk groups. (E) Nomogram predicts the probability of 3 years overall survival (OS) in CRC patients.

NOS2 knockdown. The lentiviral transfection efficiency of overexpression and knockdown was determined by qRT-PCR and western blot (Figure 6C).

Then, several experiments were performed to determine whether NOS2 affects the biological functions of CRC cells. The results of the MTT assay indicated that elevated NOS2 reduced cell proliferation, while the growth rate of cell lines increased when NOS2 was knocked down (Figure 6D).

To assess the function of NOS2 with respect to tumorigenic inhibition *in vivo*, SW620 NOS2 overexpression and control cell lines were used in subcutaneous tumorigenesis assays. The result demonstrated that elevated NOS2 expression decreased

tumorigenicity in nude mice (Figure 6E). Together, these results suggest that NOS2 mainly functions as a tumor suppressor in CRC.

NOS2 inhibits the NF-κB signaling pathway

To further demonstrate the downstream molecular mechanism of NOS2, we used GSEA software to explore the related signaling pathways in microarray data from the TCGA, GSE17538 and GSE40967. The “NF-kappa B signaling pathway”, “IL6-STAT3 signaling pathway”, “c-MYC signaling pathway” and “oxidative

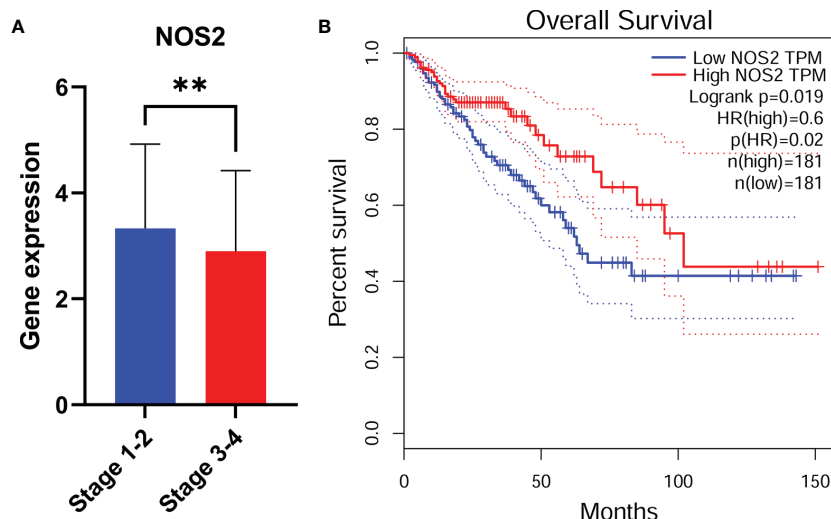


FIGURE 5

NOS2 might act as a protective factor. NOS2 expression among different tumor stage (A) in CRC. (B) CRC patients with low NOS2 expression had a shorter overall survival. **, $p < 0.01$.

phosphorylation” were highly enriched and associated with NOS2 knockdown (Figure 7A).

We initially detected the relationship between NOS2 and STAT3, c-MYC pathways. Overall, NOS2 expression does not affect p-STAT3 and c-MYC changes (Supplementary Figure 1). Therefore we explored the association of NOS2 with NF- κ B pathway.

Moreover, the western blot results suggested that NOS2 knockdown in SW480 and HCT116 cells increased the expression of p-P50 and p-P65, whereas NOS2 overexpression in SW620 and CACO2 cells reduced the expression of p-P50 and p-P65 (Figures 7B, C). Finally, to verify the regulatory relationship between NOS2 and ferroptosis, we conduct western blot and the outcome showed a higher level of GPX4 when NOS2 was knockdown, whereas NOS2 overexpression in CACO2 cells decreased the expression of GPX4 (Figures 7D, E).

In conclusion, NOS2 might inhibit CRC carcinogenicity *via* suppression of the NF- κ B signaling pathway.

Discussion

Ferroptosis is a recently discovered type of nonapoptotic mechanism involved in excessive lipid peroxidation and iron-dependent damage to membrane lipids (23, 24). Numerous studies have shown that the peroxidation of phospholipids (PLs), especially arachidonic acid, is mainly responsible for ferroptosis induction, while cumulative GPX4 and the inactivation of ACSL4 can attenuate ferroptosis by reducing lipid alcohol conversion and PL biosynthesis, respectively (24–26). At the organoid level, significant changes in mitochondrial morphology usually lead to increased membrane density, condensation or swelling and rupture of the outer membrane (27, 28).

Accumulating studies have suggested that ferroptosis participates in human diseases through a variety of mechanisms, the most likely of which is tumor suppression (23). The underlying mechanism of tumor suppression through ferroptosis in CRC remains to be investigated. In KRAS-mutant CRC cells, combination treatment with β -elemene and cetuximab enhanced the cytotoxic effect against cancer cells by inducing ferroptosis and inhibiting EMT (29). Moreover, it has been reported that the compound IMCA can upregulate SLC7A11, resulting in ROS accumulation and promoting ferroptosis (30). GPX4 is the core marker of ferroptosis, which protects cells from oxidative stress, and degradation of GPX4 contributes to ferroptosis (31). In our research, GPX4 expression was negatively correlated with the survival of CRC patients, which demonstrated the tumor inhibition effect of ferroptosis in CRC (Supplementary Figure 2). Thus, ferroptosis-inducing agents might be a potential therapeutic option for CRC treatment (32).

The exploration of ferroptosis and FRGs aimed to develop effective biomarkers for CRC prognosis prediction and therapy monitoring. In this study, we identified 8 candidates FRGs from 214 FRGs according to the FerrDb website and TCGA database and constructed a CRC predictive model. Further calculations revealed a high correlation between the survival outcomes of CRC patients and the risk score, as confirmed by uni- and multivariate Cox regression analyses. The survival rate of CRC patients in the high-risk group was significantly lower than that of CRC patients in the low-risk group, and the ROC curve for 5-year survival prediction and AUC for the risk score model showed good accuracy. These results revealed that our prognostic model, which was retrospectively validated in CRC patients at risk for mortality, had a good fit and predictive ability.

According to previous studies, the 8 FRGs selected for model construction play an important role by functionally inhibiting or promoting tumor progression in different tumor types. According to

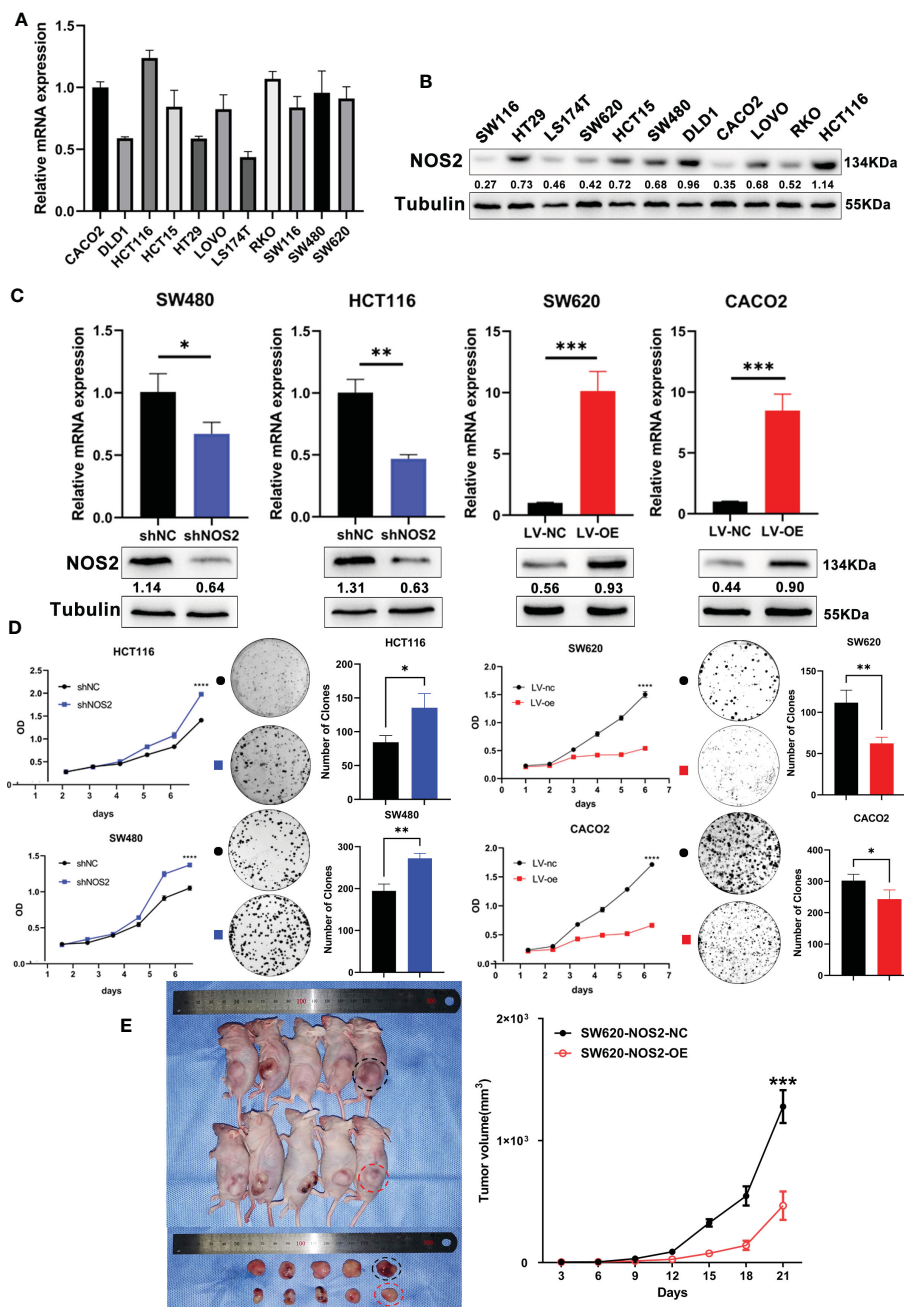


FIGURE 6 NOS2 suppresses tumor proliferation *in vitro* and *in vivo*. (A) q-PCR and (B) western blot determined the endogenous expression of NOS2 in 11 CRC cell lines. (C) q-PCR and western blot results of NOS2 expression upon knockdown and overexpression of NOS2 in different cell lines. (D) MTT assay (Left) and clonogenic assay (Right) on cell proliferation ability. (E) Subcutaneous xenograft tumor model and growth rates of tumor xenografts inoculated subcutaneously. p>0.05; *, p<0.05; **, p<0.01; ***, p<0.001.

our data, NOS2 was one of the most significantly affected FRGs, and the most obvious expression differences between high risk and low risk groups patients, therefore we began to explore the biological functions and the molecular mechanism of NOS2 in CRC. NOS2 is an inducible isoform of NOS enzymes and functions as a key inflammatory enzyme responsible for nitric oxide biosynthesis (33). Recent studies connected NOS2 and ferroptosis were almost based on bioinformatic analysis, and NOS2 had been identified as the marker of ferroptosis functions in the

process of HIF-1 signaling pathway, NOD-like receptor signaling pathway, central carbon metabolism and macrophage polarization (13, 34, 35). The dysregulation of NOS2 expression can be observed under pathological conditions, including cytokine exposure, inflammation and tumors (33, 36). A large number of studies have considered NOS2 to be a promoter and a prognostic indicator for malignancy progression. In hepatocellular carcinomas, NOS2 is a Wnt β -catenin/Tcf-4 target gene that promotes tumorigenesis (37).

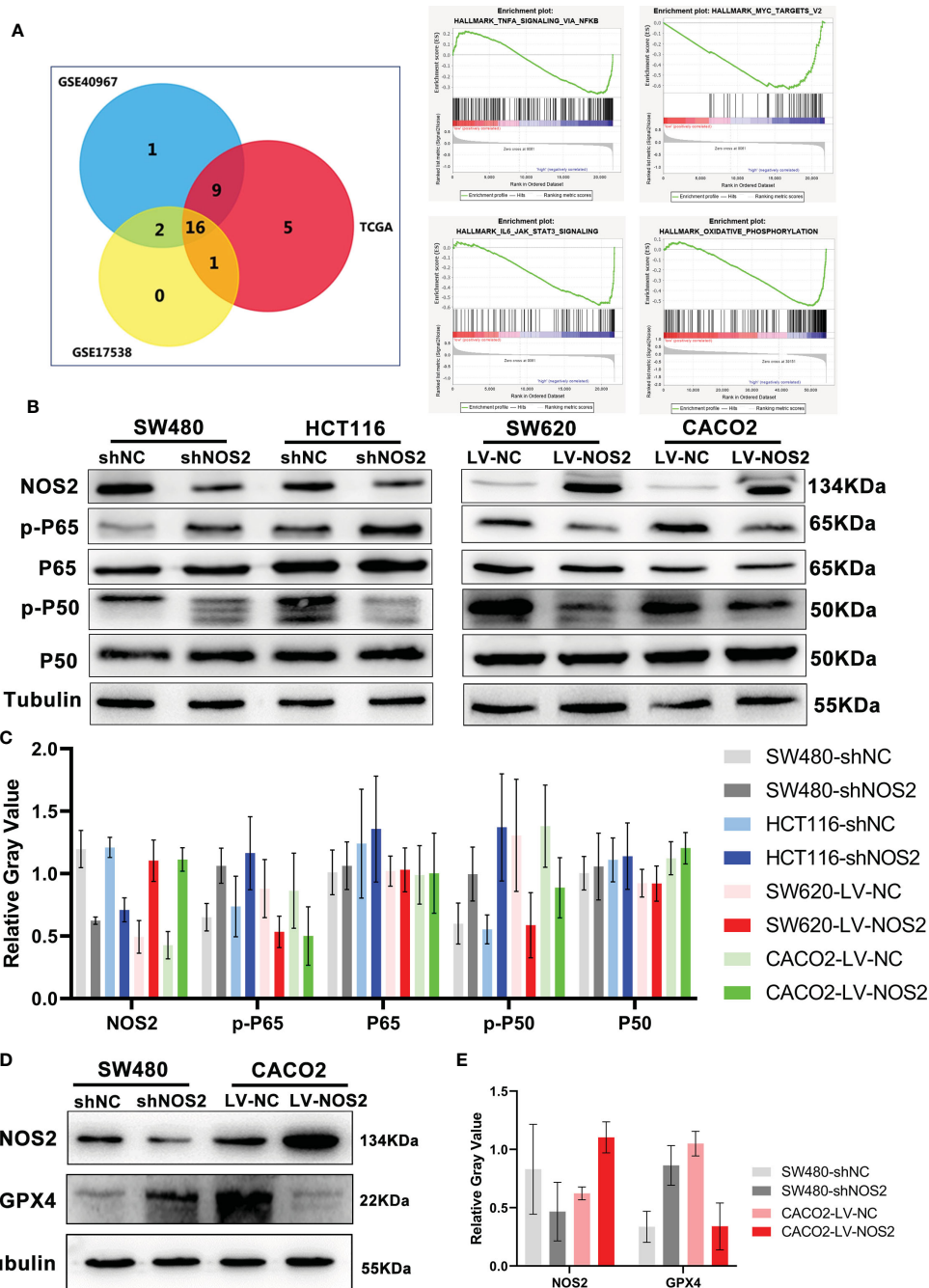


FIGURE 7
 NOS2 inhibited NF-κB signaling pathway. **(A)** The Venn figures of overlapping and different enrichment pathways between different NOS2 expression samples in 3 databases. The NF-κB signaling pathway was the most significantly enriched pathway. **(B)** NF-κB activation in different cell lines with NOS2 knockdown and overexpression was monitored by western blot analysis. **(C)** Relative expression of NOS2 and NF-κB signaling proteins. The data were expressed as the ratio of specific protein level (gray value) to Tubulin protein level (gray value). **(D)** Western blot results of GPX4 expression upon knockdown and overexpression of NOS2 in CRC cells. **(E)** Relative expression of NOS2 and GPX4.

However, NOS2 has also been proven to have both antitumor functions and tumor suppressive properties in various tumors.

It was shown that a high level of NO induced the phosphorylation and stabilization of p53 (38). In patients with ulcerative colitis or Crohn's disease, NOS2 and p-p53 are colocalized in tissues (36). Moreover, in several trials, selective or

nonselective NOS2 inhibitors did not have a therapeutic benefit in some diseases (39–41). Thus, the underlying molecular mechanisms by which NOS2 promotes the progression of CRC have remained complex and need to be further explored. In our model, considering that NOS2 was the most prominent gene and that decreased NOS2 expression was clearly linked to a poor prognosis, we performed

biological function experiments *in vitro* and *in vivo*. The results suggested that elevated NOS2 significantly inhibited CRC cell proliferation and promoted apoptosis.

Though NOS2 had been reported involving in the development of tumors in our research, the underlying molecular mechanism is still unclearly elucidated. Our further exploration of the molecular mechanism preliminarily revealed that the inhibition of NF- κ B signaling might be an important contributor to CRC when NOS2 is upregulated. In breast cancer, the co-expression of NOS2 and COX2 is involved in the regulation of oncogenic pathways such as ERK, PI3K and NF- κ B results in a poor prognosis (42, 43). Among the inflammatory diseases, NOS2 might inhibit the phosphorylation of NF- κ B (44). Our results showed that the expression level of NOS2 could induce the opposite expression of GPX4, which might demonstrate that NOS2 can participate in GPX4 synthesis or breakdown, repress NF- κ B pathway by inhibiting the phosphorylation of the p50 and p65, and thus regulated the ferroptosis in CRC cells.

Nevertheless, this study was subject to several limitations. First, it was a retrospective study, and selection bias cannot be ruled out. Second, although effective external verification was performed, internal data validation is still lacking. In addition, the molecular mechanisms underlying the 8 identified FRGs need to be further explored.

In summary, our research demonstrated, for the first time to our knowledge, the potential prognostic value of FRGs in CRC patients. The construction of a predictive model based on FRGs may be helpful for decision-making in clinical practice. In addition, our results suggest that NOS2 might inhibit CRC cell growth and induce apoptosis by inhibiting NF- κ B signaling pathways *in vitro* and *in vivo*.

Data availability statement

The original contributions presented in the study are included in the article/Supplementary Material, further inquiries can be directed to the corresponding authors.

Ethics statement

The animal study was reviewed and approved by Ethics Committee of Guangdong Provincial Hospital of Chinese Medicine.

Author contributions

XY and HL designed the study. XF, YH, and JW performed the molecular biology experiments and statistical analysis. XY, CH, and HL contributed to administrative, technical, or material support. HL and XF wrote the manuscript. All authors contributed to the article and approved the submitted version.

Funding

This study was supported by Leading Innovation Specialist Support Program of Guangdong Province, the Science and Technology Planning Project of Ganzhou (No. 202101074816), Scientific Research Project of Guangdong Provincial Traditional Chinese Medicine Bureau (No. 20211155), Medical Scientific Research Foundation of Guangdong Province (No. A2022305), National Key Clinical Specialty Construction Project (2021–2024, No. 2022YW030009), National Natural Science Foundation of China (No. 82260501), the Science and Technology Planning Project of Guangdong Provincial People's Hospital (Guangdong Academy of Medical Sciences, No. DFJH201913), CSCO-Roche Cancer Research Foundation (No. Y-2019Roche-190) and CSCO-Haosen Research Foundation (No. YHS2019/2–050).

Acknowledgments

Our authors deeply appreciate the editors and reviewers for their help with the manuscript.

Conflict of interest

The authors declare that the research was conducted in the absence of any commercial or financial relationships that could be construed as a potential conflict of interest.

Publisher's note

All claims expressed in this article are solely those of the authors and do not necessarily represent those of their affiliated organizations, or those of the publisher, the editors and the reviewers. Any product that may be evaluated in this article, or claim that may be made by its manufacturer, is not guaranteed or endorsed by the publisher.

Supplementary material

The Supplementary Material for this article can be found online at: <https://www.frontiersin.org/articles/10.3389/fonc.2023.1133946/full#supplementary-material>

SUPPLEMENTARY FIGURE 1

Different NOS2 expression level hardly affected STAT3 and c-MYC signaling pathway.

SUPPLEMENTARY FIGURE 2

Kaplan-Meier survival curves of OS with GPX4 expression level.

References

- Dekker E, Tanis PJ, Vleugels JLA, Kasi PM, Wallace MB. Colorectal cancer. *Lancet* (2019) 394(10207):1467–80. doi: 10.1016/S0140-6736(19)32319-0
- Bray F, Ferlay J, Soerjomataram I, Siegel RL, Torre LA, Jemal A. Global cancer statistics 2018: GLOBOCAN estimates of incidence and mortality worldwide for 36 cancers in 185 countries. *CA Cancer J Clin* (2018) 68(6):394–424. doi: 10.3322/caac.21492
- Arnold M, Sierra MS, Laversanne M, Soerjomataram I, Jemal A, Bray F. Global patterns and trends in colorectal cancer incidence and mortality. *Gut* (2017) 66(4):683–91. doi: 10.1136/gutjnl-2015-310912
- Sharma R. An examination of colorectal cancer burden by socioeconomic status: evidence from GLOBOCAN 2018. *EPMA J* (2020) 11(1):95–117. doi: 10.1007/s13167-019-00185-y
- Duffy MJ, Crown J. Drugging “undruggable” genes for cancer treatment: are we making progress? *Int J Cancer* (2020) 148(1):8–17. doi: 10.1002/ijc.33197
- Sveen A, Kopetz S, Lothe RA. Biomarker-guided therapy for colorectal cancer: strength in complexity. *Nat Rev Clin Oncol* (2020) 17(1):11–32. doi: 10.1038/s41571-019-0241-1
- Dixon SJ, Lemberg KM, Lamprecht MR, Skouta R, Zaitsev EM, Gleason CE, et al. Ferroptosis: an iron-dependent form of nonapoptotic cell death. *Cell* (2012) 149(5):1060–72. doi: 10.1016/j.cell.2012.03.042
- Liang C, Zhang X, Yang M, Dong X. Recent progress in ferroptosis inducers for cancer therapy. *Adv Mater* (2019) 31(51):e1904197. doi: 10.1002/adma.201904197
- Xie Y, Zhu S, Song X, Sun X, Fan Y, Liu J, et al. The tumor suppressor p53 limits ferroptosis by blocking DPP4 activity. *Cell Rep* (2017) 20(7):1692–704. doi: 10.1016/j.celrep.2017.07.055
- Chen P, Li X, Zhang R, Liu S, Xiang Y, Zhang M, et al. Combinative treatment of beta-elemene and cetuximab is sensitive to KRAS mutant colorectal cancer cells by inducing ferroptosis and inhibiting epithelial-mesenchymal transformation. *Theranostics* (2020) 10(11):5107–19. doi: 10.7150/thno.44705
- Zhang Y, Song J, Zhao Z, Yang M, Chen M, Liu C, et al. Single-cell transcriptome analysis reveals tumor immune microenvironment heterogeneity and granulocytes enrichment in colorectal cancer liver metastases. *Cancer Lett* (2020) 470:84–94. doi: 10.1016/j.canlet.2019.10.016
- Chapkin RS, Navarro SL, Hullar MAJ, Lampe JW. Diet and gut microbes act coordinately to enhance programmed cell death and reduce colorectal cancer risk. *Dig Dis Sci* (2020) 65(3):840–51. doi: 10.1007/s10620-020-06106-8
- He J, Li X, Yu M. Bioinformatics analysis identifies potential ferroptosis key genes in the pathogenesis of pulmonary fibrosis. *Front Genet* (2021) 12:788417. doi: 10.3389/fgenet.2021.788417
- Chen Y, Li H. Prognostic and predictive models for left- and right- colorectal cancer patients: a bioinformatics analysis based on ferroptosis-related genes. *Front Oncol* (2022) 12:833834. doi: 10.3389/fonc.2022.833834
- Vannini F, Kashfi K, Nath N. The dual role of iNOS in cancer. *Redox Biol* (2015) 6:334–43. doi: 10.1016/j.redox.2015.08.009
- Somasundaram V, Gilmore AC, Basudhar D, Palmieri EM, Scheiblin DA, Heinz WF, et al. Inducible nitric oxide synthase-derived extracellular nitric oxide flux regulates proinflammatory responses at the single cell level. *Redox Biol* (2020) 28:2213–17. doi: 10.1016/j.redox.2019.101354
- Perwez Hussain S. Deciphering the complex biological interactions of nitric oxide in cancer. *Redox Biol* (2015) 5:413. doi: 10.1016/j.redox.2015.09.011
- Thomas DD, Wink DA. NOS2 as an emergent player in progression of cancer. *Antioxid Redox Signal* (2017) 26(17):963–5. doi: 10.1089/ars.2016.6835
- Fransen K, Elander N, Soderkvist P. Nitric oxide synthase 2 (NOS2) promoter polymorphisms in colorectal cancer. *Cancer Lett* (2005) 225(1):99–103. doi: 10.1016/j.canlet.2005.02.006
- Speckmann B, Pinto A, Winter M, Förster I, Sies H, Steinbrenner H. Proinflammatory cytokines down-regulate intestinal selenoprotein P biosynthesis via NOS2 induction. *Free Radic Biol Med* (2010) 49(5):777–85. doi: 10.1016/j.freeradbiomed.2010.05.035
- Marigo I, Zilio S, Desantis G, Mlecnik B, Agnellini AH, Ugel S, et al. T Cell cancer therapy requires CD40-CD40L activation of tumor necrosis factor and inducible nitric-oxide-synthase-producing dendritic cells. *Cancer Cell* (2016) 30(4):651. doi: 10.1016/j.ccell.2016.09.009
- Zhu Y, Wang R, Chen W, Chen Q, Zhou J. Construction of a prognosis-predicting model based on autophagy-related genes for hepatocellular carcinoma (HCC) patients. *Aging (Albany NY)* (2020) 12(14):14582–92. doi: 10.18632/aging.103507
- Stockwell BR, Jiang X, Gu W. Emerging mechanisms and disease relevance of ferroptosis. *Trends Cell Biol* (2020) 30(6):478–90. doi: 10.1016/j.tcb.2020.02.009
- Lei G, Zhang Y, Koppula P, Liu X, Zhang J, Lin SH, et al. The role of ferroptosis in ionizing radiation-induced cell death and tumor suppression. *Cell Res* (2020) 30(2):146–62. doi: 10.1038/s41422-019-0263-3
- Kagan VE, Mao G, Qu F, Angeli JP, Doll S, Croix CS, et al. Oxidized arachidonic and adrenic PES navigate cells to ferroptosis. *Nat Chem Biol* (2017) 13(1):81–90. doi: 10.1038/nchembio.2238
- Seibt TM, Proneth B, Conrad M. Role of GPX4 in ferroptosis and its pharmacological implication. *Free Radic Biol Med* (2019) 133:144–52. doi: 10.1016/j.freeradbiomed.2018.09.014
- Tang D, Chen X, Kang R, Kroemer G. Ferroptosis: molecular mechanisms and health implications. *Cell Res* (2020). doi: 10.1038/s41422-020-00441-1
- Gao M, Yi J, Zhu J, Minikes AM, Monian P, Thompson CB, et al. Role of mitochondria in ferroptosis. *Mol Cell* (2019) 73(2):354–363 e353. doi: 10.1016/j.molcel.2018.10.042
- Chen P, Li X, Zhang R, Liu S, Xiang Y, Zhang M, et al. Combinative treatment of beta-elemene and cetuximab is sensitive to KRAS mutant colorectal cancer cells by inducing ferroptosis and inhibiting epithelial-mesenchymal transformation. (2020) 10(11):5107–19. doi: 10.7150/thno.44705
- Zhang L, Liu W, Liu F, Wang Q, Song M, Yu Q, et al. Corrigendum to “IMCA induces ferroptosis mediated by SLC7A11 through the AMPK/mTOR pathway in colorectal cancer”. (2020) 2020:6901472. doi: 10.1155/2020/6901472
- Ursini F, Maiorino M. Lipid peroxidation and ferroptosis: the role of GSH and GPx4. *Free Radic Biol Med* (2020) 152:175–85. doi: 10.1016/j.freeradbiomed.2020.02.027
- Weigand I, Schreiner J, Röhrig F, Sun N, Landwehr LS, Urlaub H, et al. Active steroid hormone synthesis renders adrenocortical cells highly susceptible to type II ferroptosis induction. *Cell Death Dis.* (2020) 11(3):192. doi: 10.1038/s41419-020-2385-4
- Basudhar D, Bharadwaj G, Somasundaram V, Cheng RYS, Ridnour LA, Fujita M, et al. Understanding the tumour micro-environment communication network from an NOS2/COX2 perspective. *Br J Pharmacol* (2018) 176(2):155–76. doi: 10.1111/bph.14488
- Fujii J, Osaki T. Involvement of nitric oxide in protecting against radical species and autoregulation of M1-polarized macrophages through metabolic remodeling. *Molecules* (2023) 28(2). doi: 10.3390/molecules28020814
- Sun S, Wu Y, Maimaitijiang A, Huang Q, Chen Q. Ferroptotic cardiomyocyte-derived exosomes promote cardiac macrophage M1 polarization during myocardial infarction. *PeerJ* (2022) 10:e13717. doi: 10.7717/peerj.13717
- Thomas DD, Heinecke JL, Ridnour LA, Cheng RY, Kesarwala AH, Switzer CH, et al. Signaling and stress: the redox landscape in NOS2 biology. *Free Radic Biol Med* (2015) 87:204–25. doi: 10.1016/j.freeradbiomed.2015.06.002
- Wang R, Geller DA, Wink DA, Cheng B, Billiar TR. NO and hepatocellular cancer. *Br J Pharmacol.* (2020) 177(24):5459–66. doi: 10.1111/bph.14838
- Hofseth LJ, Saito S, Hussain SP, Espey MG, Miranda KM, Araki Y, et al. Nitric oxide-induced cellular stress and p53 activation in chronic inflammation. *Proc Natl Acad Sci USA* (2003) 100(1):143–8. doi: 10.1073/pnas.0237083100
- Dzavik V, Cotter G, Reynolds HR, Alexander JH, Ramanathan K, Stebbins AL, et al. Effect of nitric oxide synthase inhibition on haemodynamics and outcome of patients with persistent cardiogenic shock complicating acute myocardial infarction: a phase II dose-ranging study. *Eur Heart J.* (2007) 28(9):1109–16. doi: 10.1093/eurheartj/ehm075
- Hansel TT, Kharitonov SA, Donnelly LE, Erin EM, Currie MG, Moore WM, et al. A selective inhibitor of inducible nitric oxide synthase inhibits exhaled breath nitric oxide in healthy volunteers and asthmatics. *FASEB J.* (2003) 17(10):1298–300. doi: 10.1096/fj.02-0633fje
- Hellio le Graverand MP, Clemmer RS, Redifer P, Brunell RM, Hayes CW, Brandt KD, et al. A 2-year randomised, double-blind, placebo-controlled, multicentre study of oral selective iNOS inhibitor, cindunistat (SD-6010), in patients with symptomatic osteoarthritis of the knee. *Ann Rheum Dis.* (2013) 72(2):187–95. doi: 10.1136/annrheumdis-2012-202239
- Basudhar D, Glynn SA, Greer M, Somasundaram V, No JH, Scheiblin DA, et al. Coexpression of NOS2 and COX2 accelerates tumor growth and reduces survival in estrogen receptor-negative breast cancer. *Proc Natl Acad Sci USA* (2017) 114(49):13030–5. doi: 10.1073/pnas.1709119114
- Glynn SA, Boersma BJ, Dorsey TH, Yi M, Yfantis H, Ridnour L, et al. Increased NOS2 predicts poor survival in estrogen receptor-negative breast cancer patients. *J Clin Invest.* (2010) 120(11):3843–54. doi: 10.1172/JCI42059
- Wei X, Zhang B, Liang X, Liu C, Xia T, Xie Y, et al. Higenamine alleviates allergic rhinitis by activating AKT1 and suppressing the EGFR/JAK2/c-JUN signaling. *Phytomedicine* (2021) 86:153565. doi: 10.1016/j.phymed.2021.153565